

Weights Decision Analysis on the Integration of Navigation Satellite System and Vision System for Precise Positioning

Chi-Ho Park, Nam-Hyeok Kim

IT Convergence Division

DGIST

Daegu, S.Korea

{chpark, nhkim}@dgist.ac.

Abstract— In this paper, we propose a precise and reliable positioning method for solving common problems, such as a navigation satellite's signal occlusion in an urban canyon and the positioning error due to a limited number of visible navigation satellites. This is an integrated system of the navigation satellites system and a vision system. In general, the navigation satellite positioning system has a fatal weakness in that it cannot calculate a position coordinate when its signal is occluded by some obstacle. For this reason, positioning by the navigation satellites system cannot be used for a variety of applications. Therefore, we propose a method to integrate both the navigation satellites system and a vision system using weights decision analysis for precise positioning.

Keywords-GNSS; Vision; Integration; Positioning.

I. INTRODUCTION

The Global Positioning System (GPS) was developed in the United States for military purposes. However, in the 1990s, after being opened to the private sector, it has become widely used for vehicle navigation, aircraft, communications, science, agriculture, and exploration. In addition, the Soviet Union's navigation satellite system GLONASS was also opened to the private sector and this has allowed the Global Navigation Satellite System (GNSS) to be utilized for more purposes. Recently, there have been a lot of studies involving GNSS applications [1]-[3]. The advantages of this system include improved position accuracy, convenience, continuity, continuous usability, integrity, and so on. The most important feature of GNSS is its frequency band allocation. Consultations regarding spectrum allocation have assigned the L1 band to 1575.42MHz, the L2 band to 1227.60MHz, and the L5 band to 1176.45MHz in the WRC2000. An increase in the satellites and multi-frequency have solved problems, such as poor accuracy and continuity, however rapidly developing industrialization has increased many of these problems. In particular, the increased position error due to cycle slip and multipath exacerbates these problems. Further, many areas of the earth outdoors are still in a GPS shadow. These factors are the main cause of decreased reliability and continuity [4].

Today's navigation satellite system provides location information services within around 100 m (drms) accuracy at any time, regardless of the number of users. The system calculates a three-dimensional position by using triangulation, so it can be operated whenever the receiver can take signals

from more than 4 satellites. However, locations in a city or in mountainous areas cannot always receive satellite signals because they may be blocked by high buildings or mountains. In such cases, the position error will be bigger or shaded areas will occur. Consequently, to solve these problems, many researchers have proposed techniques using the navigation satellite system and other applications [5]-[6].

One representative research is an integration system involving the navigation satellite system and an Inertial Measurement Unit (IMU). This system is a device used by countries to detect the location of their own submarines, aircraft, missiles, etc. and to drive to a targeted destination. The operating principle involves calculating the moving variance by using accelerometers, after determining cardinal points by gyroscope. The moving object can always calculate its current position and velocity after being input with the initial position. The advantage of IMU is that it is not affected by weather or jamming. However, when moving over a long distance, errors are accumulated. So, GPS correction is needed. In the case that signals are not received from satellites, the errors of the IMU are exponentially increased. Therefore, factors which cause shaded areas and obstacles limit the uses of kinematic positioning [7]. Due to rapid industrialization, the areas and environments where the navigation satellite system can be used is being reduced by the increasing growth of urban canyons. Fig. 1 shows a general situation for navigation satellite system signal reception in an urban canyon.

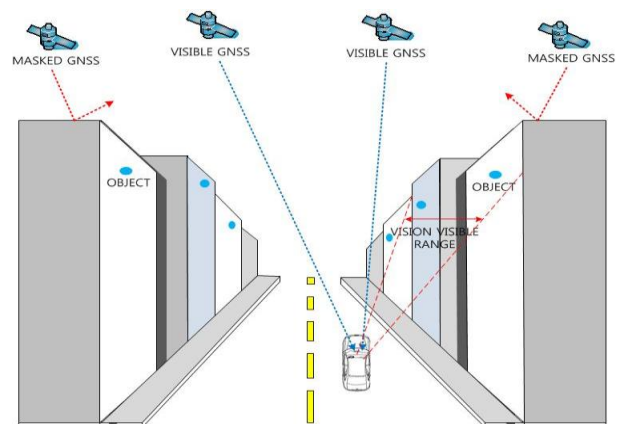


Figure 1. The situation for signal reception from the navigation satellite in an urban canyon.

Recently, a vision system was reported at a DARPA unmanned vehicle conference in the United States, which, in part, dealt with obstacle recognition and detection [8]-[9]. In particular, one team reported that they had used only a vision system for detection and recognition. But the vision system had some constraints, such as a real time processing problem due to the large amounts of data, and a recognition error due to external lighting changes.

Other recent researches using a vision system have made a lot of progress by improving the computer's performance and data processing time through the development of integration technology and the development of a broadband camera [10]-[11].

The advantages of the vision system are its wide range and long detection distance, the ease of data processing due to its similarity with the human visual system, and the provision of a variety of information. A stereo vision system that is capable of solving many of the problems of a monocular vision system uses a stereo matching algorithm for extracting a depth map, and an obstacle detection algorithm based on this depth map [12].

Therefore, in this paper, we propose a method to integrate both the navigation satellite system and the vision system using a weights decision analysis for precise positioning.

This paper explains the problems of the existing fusion research and the limitations of positioning using a satellite navigation system in the Introduction. In the main part it proposes an equation and description for the fusion algorithm of the satellite navigation system and vision system. The performance analysis presents a comparative experiment and analysis of the integration of the navigation satellite system and vision system for precise positioning using weights decision.

II. ALGORITHM

A. Positioning using a navigation satellite system

Usually, the position is obtained in point positioning mode by using a receiver chip that is mounted on the vehicle which receives the L1 C/A (Coarse/Acquisition) code from the navigation satellites. The C/A code observation equation for the navigation satellites system is given as follows.

$$P_{i,1}^k = \rho_i^k + T_i^k + \frac{I_i^k}{f_1^2} + c(dt_i - dt^k) + e_{i,1}^k$$

$$\rho_i^k = \sqrt{(x^k - x_i)^2 + (y^k - y_i)^2 + (z^k - z_i)^2} \quad (1)$$

where, i and k denote receiver and satellite, respectively.

$P_{i,1}^k$: L1 C/A code pseudorange between the receiver and the satellite (m);

ρ_i^k : actual geometric distance between receiver and satellite (m);

T_i^k : tropospheric delay error (m);

$\frac{I_i^k}{f_1^2}$: ionospheric delay error (m);

C : speed of light (m/s);

dt_i : receiver clock error (sec);

dt^k : satellite clock error (sec);

$e_{i,1}^k$: measurement error.

Ionospheric delay effects and satellite clock errors are removed by a navigation message from the satellites. Tropospheric delay effects are removed by models that account for the dry and wet refractivity at the surface of the Earth. Multipath error is not assumed. Inter-frequency bias is ignored because of its small value. As a consequence, (2) can be used for the observation equation to compute the receiver's position in 3-dimensional space.

$$PG_{i,1}^k - T_i^k - \frac{I_i^k}{f_1^2} + cdt^k = \rho_i^k + cdt_i + e_{i,1}^k \quad (2)$$

We denote by $P_{i,c}^k$ in the left side of (2) and linearize (2) because it is a non-linear equation. After that, the Gauss-Markov Model (GMM) [13] is applied. The result is (3). The satellites' position coordinates are determined by using the navigation message. Unknown factors are the 3-dimensional position and receiver clock error.

$$y = A\xi + e, \quad e \sim (0, \sigma_0^2 P^{-1}) \quad (3)$$

Each item is shown below, $\dot{\rho}$ is calculated by the receiver's initial position $(\dot{x}_i, \dot{y}_i, \dot{z}_i)$.

$$y = \begin{bmatrix} P_{i,0}^k & - & P_{i,c}^k \\ P_{i,0}^l & - & P_{i,c}^l \\ \vdots & & \\ P_{i,0}^q & & P_{i,c}^q \end{bmatrix} : \text{Observation vector}$$

$$A = \begin{bmatrix} -\frac{x^k - \dot{x}_i}{\dot{\rho}_i^k} - \frac{y^k - \dot{y}_i}{\dot{\rho}_i^k} - \frac{z^k - \dot{z}_i}{\dot{\rho}_i^k} & c \\ -\frac{x^l - \dot{x}_i}{\dot{\rho}_i^l} - \frac{y^l - \dot{y}_i}{\dot{\rho}_i^l} - \frac{z^l - \dot{z}_i}{\dot{\rho}_i^l} & c \\ \vdots & \\ -\frac{x^q - \dot{x}_i}{\dot{\rho}_i^q} - \frac{y^q - \dot{y}_i}{\dot{\rho}_i^q} - \frac{z^q - \dot{z}_i}{\dot{\rho}_i^q} & c \end{bmatrix} : \text{Design matrix}$$

$$\xi = \begin{bmatrix} \Delta x_i \\ \Delta y_i \\ \Delta z_i \\ dt_i \end{bmatrix} : \text{Unknown parameter vector}$$

$$e = \begin{bmatrix} e_i^k \\ e_i^l \\ \vdots \\ e_i^q \end{bmatrix} : \text{Measurement error vector}$$

$n \times 1$

The unknown that is calculated in (3) is the increment with respect to the initial value.

$$\hat{\xi} = \underbrace{(A^T P A)^{-1}}_N A^T P y \quad (4)$$

The increment from (4) is added to the receiver's initial position and then the receiver's position is updated. This process is iterated until the increment is under the particular threshold value. After this process, the receiver's position is determined.

$$\begin{bmatrix} X_i \\ Y_i \\ Z_i \end{bmatrix}_{\text{update}} = \begin{bmatrix} X_i \\ Y_i \\ Z_i \end{bmatrix}_{\text{initial}} + \begin{bmatrix} \Delta X_i \\ \Delta Y_i \\ \Delta Z_i \end{bmatrix} \quad (5)$$

The variance component can be computed by using (6). Also, the variance-covariance matrix for the estimates can be obtained using (7).

$$\hat{\sigma}_0^2 = \frac{\tilde{e}^T P \tilde{e}}{n - rKA} \quad (6)$$

where, $\tilde{e} = y - A\hat{\xi}$, n is the number of observations.

$$D\{\hat{\xi}\} = \hat{\sigma}_0^2 N^{-1} \quad (7)$$

B. Fusion positioning equations

The vision system obtains observation values by recognizing objects. This means that the sizes of the observation vector and design matrix get larger as the number of observations increases. The distance from the receiver to the target object can be computed by using the vision system and the corresponding observation equation is as follows.

$$PV_i^a = \rho_i^a + e_i^a$$

$$\rho_i^a = \sqrt{(x^a - x_i)^2 + (y^a - y_i)^2 + (z^a - z_i)^2} \quad (8)$$

PV_i^a : distance estimated by the vision system from the specific object to the receiver (m).

ρ_i^a : actual distance from the specific object to the receiver.

x^a, y^a, z^a : three-dimensional position of a specific object.

x_i, y_i, z_i : three-dimensional position of the receiver.

After linearization, (9) can be rewritten as follows.

$$z_0 = K\xi + e_0, \quad e_0 \sim (\sigma_0^2 P_0^{-1}) \quad (9)$$

$$Z_0 = \underbrace{[PV_i^a \dots \rho_i^a]}_{1 \times 1} : \text{Observation vector}$$

$$A = \begin{bmatrix} -\frac{x^a - x_i}{\rho_i^a} - \frac{y^a - y_i}{\rho_i^a} - \frac{z^a - z_i}{\rho_i^a} & 0 \end{bmatrix} : \text{Design matrix}$$

$$\xi = \begin{bmatrix} \Delta x_i \\ \Delta y_i \\ \Delta z_i \\ dt_i \end{bmatrix} : \text{Unknown parameter vector}$$

The distance measurement from the vision system can be used as an additional observation and then the Gauss-Markov adjustment model with stochastic constraints is applied as shown in (10).

$$\hat{\xi} = (N + K^T P_0 K)^{-1} (c + K^T P_0 z_0) \quad (10)$$

The residual of the distance estimated by the vision system is $e_0 = Z_0 - K\xi$ and the estimated variance component is (11).

$$\hat{\sigma}_0^2 = \frac{\tilde{e}^T P \tilde{e} + \tilde{e}_0^T P_0 \tilde{e}_0}{n - m + l} \quad (11)$$

Here, n is the observed number of navigation satellites, m is the number of unknown parameters (coordinates 3, receiver's clock error 1), l is the number of the distance measurement obtained from the vision system. Also, the variance-covariance matrix for the estimates can be computed by using (12).

$$D\{\hat{\xi}\} = \hat{\sigma}_0^2 (N + K^T P_0 K)^{-1} \quad (12)$$

where, a is the specific object, i is a receiver, and each of the items are as follow.

PV_i^a : distance estimated by the vision system from the specific object to the receiver (m).

ρ_i^a : actual distance from the specific object to the receiver.

x^a, y^a, z^a : three-dimensional position of a specific object.

x_i, y_i, z_i : three-dimensional position of the receiver.

III. PERFORMANCE ANALYSIS

Experiments were conducted to evaluate the reliability and stability of positioning based on the integration of the navigation satellites system and the vision system. The

receiver of the navigation satellite system was the DL-V3 Real Time Kinematic (RTK) of Novatel for the base station and the rover. The antenna was GPS-702-GGL of Novatel, the RF modem was the PDL rover kit of 450 MHz, and the Inertial Measurement Unit (IMU) was CG-5100 of KVH. Also, a stereo camera was used as the image sensor. The focal length of the image sensor was 12 mm and the baseline of the stereo camera (x coordinate difference between the two cameras) was 300 mm.

We compared the static and kinematic states of a vehicle in the experiments.

The following are results of experiments in the static state. Figure 2 shows the sky plot of the static state.

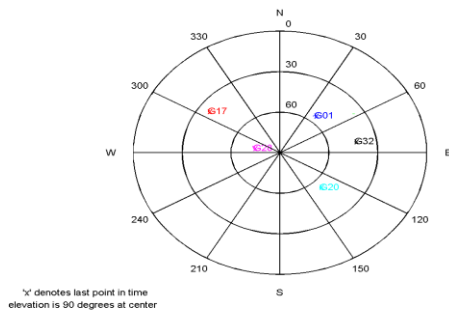


Figure 2. Sky plot.

Tables I-VIII show the Horizontal Positioning Error according to the variance of number of satellites and vision’s target object. (In the tables, G means the number of visible navigation satellites and V means the number of target objects for the vision system. For example, G3V1 means that there are 3 navigation satellites and one vision target object.)

Table I shows the Horizontal Position Error when there are three visible navigation satellites, and the number of target objects for the vision system is one.

TABLE I. HORIZONTAL POSITION ERROR

| G3+V1 | | |
|--------------------|----------------------|-------------------------|
| <i>GNSS Weight</i> | <i>Vision Weight</i> | <i>Horizontal Error</i> |
| 1 | 1 | 19.96 |
| 1 | 2 | 19.89 |
| 1 | 3 | 20.05 |
| 1 | 5 | 20.41 |
| 1 | 10 | 19.87 |
| 2 | 1 | 19.83 |
| 3 | 1 | 20.30 |
| 5 | 1 | 20.22 |
| 10 | 1 | 19.84 |

Table II shows the Horizontal Position Error with three visible navigation satellites, and the number of target objects for the vision system is two.

TABLE II. HORIZONTAL POSITION ERROR

| G3+V2 | | |
|--------------------|----------------------|-------------------------|
| <i>GNSS Weight</i> | <i>Vision Weight</i> | <i>Horizontal Error</i> |
| 1 | 1 | 13.47 |
| 1 | 2 | 16.59 |
| 1 | 3 | 17.62 |
| 1 | 5 | 18.18 |
| 1 | 10 | 18.45 |
| 2 | 1 | 10.29 |
| 3 | 1 | 9.37 |
| 5 | 1 | 8.90 |
| 10 | 1 | 9.10 |

Table III shows the Horizontal Position Error with three visible navigation satellites, and the number of target objects for the vision system is three.

TABLE III. HORIZONTAL POSITION ERROR

| G3+V3 | | |
|--------------------|----------------------|-------------------------|
| <i>GNSS Weight</i> | <i>Vision Weight</i> | <i>Horizontal Error</i> |
| 1 | 1 | 13.17 |
| 1 | 2 | 16.11 |
| 1 | 3 | 17.17 |
| 1 | 5 | 17.85 |
| 1 | 10 | 18.17 |
| 2 | 1 | 10.34 |
| 3 | 1 | 9.06 |
| 5 | 1 | 7.69 |
| 10 | 1 | 6.42 |

Table IV shows the Horizontal Position Error with four visible navigation satellites, and the number of target objects for the vision system is zero.

TABLE IV. HORIZONTAL POSITION ERROR

| G4 |
|-------------------------|
| <i>Horizontal Error</i> |
| 24.42 |

Table V shows the Horizontal Position Error with four visible navigation satellites, and the number of target objects for the vision system is one.

TABLE V. HORIZONTAL POSITION ERROR

| G4+V1 | | |
|--------------------|----------------------|-------------------------|
| <i>GNSS Weight</i> | <i>Vision Weight</i> | <i>Horizontal Error</i> |
| 1 | 1 | 19.83 |
| 1 | 2 | 20.04 |
| 1 | 3 | 19.35 |
| 1 | 5 | 19.62 |
| 1 | 10 | 20.58 |
| 2 | 1 | 19.46 |
| 3 | 1 | 19.42 |
| 5 | 1 | 19.26 |
| 10 | 1 | 19.32 |

Table VI shows the Horizontal Position Error with four visible navigation satellites, and the number of target objects for the vision system is two.

TABLE VI. HORIZONTAL POSITION ERROR

| G4+V2 | | |
|--------------------|----------------------|-------------------------|
| <i>GNSS Weight</i> | <i>Vision Weight</i> | <i>Horizontal Error</i> |
| 1 | 1 | 13.67 |
| 1 | 2 | 18.01 |
| 1 | 3 | 19.43 |
| 1 | 5 | 20.52 |
| 1 | 10 | 21.37 |
| 2 | 1 | 10.26 |
| 3 | 1 | 8.64 |
| 5 | 1 | 7.77 |
| 10 | 1 | 7.51 |

Table VII shows the Horizontal Position Error with four visible navigation satellites, and the number of target objects for the vision system is three.

TABLE VII. HORIZONTAL POSITION ERROR

| G4+V3 | | |
|--------------------|----------------------|-------------------------|
| <i>GNSS Weight</i> | <i>Vision Weight</i> | <i>Horizontal Error</i> |
| 1 | 1 | 13.61 |
| 1 | 2 | 15.68 |
| 1 | 3 | 16.28 |
| 1 | 5 | 16.73 |
| 1 | 10 | 21.79 |
| 2 | 1 | 10.63 |
| 3 | 1 | 9.10 |
| 5 | 1 | 7.60 |
| 10 | 1 | 6.39 |

Table VIII shows the Horizontal Position Error with five visible navigation satellites, and the number of target objects for the vision system is zero.

TABLE VIII. HORIZONTAL POSITION ERROR

| G5 |
|-------------------------|
| <i>Horizontal Error</i> |
| 28.15 |

The following are results of experiments in the kinematic state. Figure 3 shows the kinematic state sky plot.

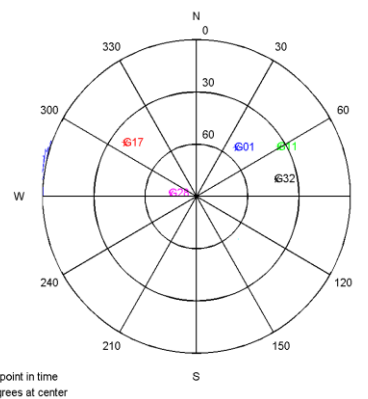


Figure 3. Sky plot of kinematic state.

Tables IX-XVI show the Horizontal Positioning Error according to the variance of number of satellites and vision's target object.

Table IX shows the Horizontal Position Error with three visible navigation satellites, and the number of target objects for the vision system is one.

TABLE IX. HORIZONTAL POSITION ERROR

| G3+V1 | | |
|--------------------|----------------------|-------------------------|
| <i>GNSS Weight</i> | <i>Vision Weight</i> | <i>Horizontal Error</i> |
| 1 | 1 | 21.62 |
| 1 | 2 | 21.02 |
| 1 | 3 | 21.96 |
| 1 | 5 | 20.32 |
| 1 | 10 | 20.33 |
| 2 | 1 | 21.67 |
| 3 | 1 | 20.99 |
| 5 | 1 | 20.50 |
| 10 | 1 | 20.34 |

Table X shows the Horizontal Position Error with three visible navigation satellites, and the number of target objects for the vision system is two.

TABLE X. HORIZONTAL POSITION ERROR

| G3+V2 | | |
|--------------------|----------------------|-------------------------|
| <i>GNSS Weight</i> | <i>Vision Weight</i> | <i>Horizontal Error</i> |
| 1 | 1 | 23.95 |
| 1 | 2 | 19.94 |
| 1 | 3 | 19.68 |
| 1 | 5 | 20.06 |
| 1 | 10 | 20.25 |
| 2 | 1 | 17.57 |
| 3 | 1 | 20.65 |
| 5 | 1 | 16.68 |
| 10 | 1 | 17.43 |

Table XI shows the Horizontal Position Error with three visible navigation satellites, and the number of target objects for the vision system is three.

TABLE XI. HORIZONTAL POSITION ERROR

| G3+V3 | | |
|--------------------|----------------------|-------------------------|
| <i>GNSS Weight</i> | <i>Vision Weight</i> | <i>Horizontal Error</i> |
| 1 | 1 | 18.07 |
| 1 | 2 | 18.88 |
| 1 | 3 | 19.29 |
| 1 | 5 | 22.05 |
| 1 | 10 | 19.93 |
| 2 | 1 | 16.13 |
| 3 | 1 | 18.96 |
| 5 | 1 | 13.30 |
| 10 | 1 | 12.75 |

Table XII shows the Horizontal Position Error with four visible navigation satellites, and the number of target objects for the vision system is zero.

TABLE XII. HORIZONTAL POSITION ERROR

| G4 |
|-------------------------|
| <i>Horizontal Error</i> |
| 20.95 |

Table XIII shows the Horizontal Position Error with four visible navigation satellites, and the number of target objects for the vision system is one.

TABLE XIII. HORIZONTAL POSITION ERROR

| G4+V1 | | |
|--------------------|----------------------|-------------------------|
| <i>GNSS Weight</i> | <i>Vision Weight</i> | <i>Horizontal Error</i> |
| 1 | 1 | 13.86 |
| 1 | 2 | 23.18 |
| 1 | 3 | 17.52 |
| 1 | 5 | 20.26 |
| 1 | 10 | 20.78 |
| 2 | 1 | 24.86 |
| 3 | 1 | 24.10 |
| 5 | 1 | 13.24 |
| 10 | 1 | 24.82 |

Table XIV shows the Horizontal Position Error with four visible navigation satellites, and the number of target objects for the vision system is two.

TABLE XIV. HORIZONTAL POSITION ERROR

| G4+V2 | | |
|--------------------|----------------------|-------------------------|
| <i>GNSS Weight</i> | <i>Vision Weight</i> | <i>Horizontal Error</i> |
| 1 | 1 | 22.86 |
| 1 | 2 | 22.94 |
| 1 | 3 | 21.67 |
| 1 | 5 | 18.97 |
| 1 | 10 | 20.66 |
| 2 | 1 | 21.15 |
| 3 | 1 | 19.21 |
| 5 | 1 | 12.45 |
| 10 | 1 | 11.49 |

Table XV shows the Horizontal Position Error with four visible navigation satellites, and the number of target objects for the vision system is three.

TABLE XV. HORIZONTAL POSITION ERROR

| G4+V3 | | |
|--------------------|----------------------|-------------------------|
| <i>GNSS Weight</i> | <i>Vision Weight</i> | <i>Horizontal Error</i> |
| 1 | 1 | 22.28 |
| 1 | 2 | 22.64 |
| 1 | 3 | 21.50 |
| 1 | 5 | 18.65 |
| 1 | 10 | 19.53 |
| 2 | 1 | 19.56 |
| 3 | 1 | 16.57 |
| 5 | 1 | 7.45 |
| 10 | 1 | 6.29 |

Table XVI shows the Horizontal Position Error with five visible navigation satellites, and the number of target objects for the vision system is zero.

TABLE XVI. HORIZONTAL POSITION ERROR

| G5 | |
|-------------------------|--|
| <i>Horizontal Error</i> | |
| 16.33 | |

IV. CONCLUSION AND FUTURE WORK

Tables I-VII show the Horizontal Positioning Error according to the variance of number of satellites and vision's target object. The experimental results in Tables I-III and VIII-X indicate that the position could be determined with the addition of the vision system when there was less than four visible satellites. In Tables I-III, we can confirm that the results using three visible satellites with one, two, and three visual target objects are better than when using four visible satellites without the vision system. The performance of Horizontal Position Error was improved 19%, 64%, and 74%. In Tables V-VII, we can confirm that the results using four visible satellites with one, two, and three visual target objects are better than when using five visible satellites without the vision system. The performance of Horizontal Position Error was improved 32%, 74%, and 78%. In Tables IX-XI, we can confirm that the results using three visible satellites with one, two, and three visual target objects are better than using four visible satellites without the vision system. The performance of Horizontal Position Error was improved 0.4%, 21%, and 40%. In Tables XIII-XV, we can confirm that the results using four visible satellites with one, two, and three visual target objects are better than when using five visible satellites without the vision system. The performance of Horizontal Position Error was improved 19%, 21%, and 40%.

ACKNOWLEDGEMENT

This work was supported by the DGIST R&D Program of the Ministry of Science, ICT & Future Planning of Korea. (14-IT-01)

REFERENCES

- [1] J. B. Tsui, "Fundamentals of Global System Receivers, A Software Approach", John Wiley & Sons, 2. 2000, pp. 10-27.
- [2] P. Ramjee and R. Marina, "Applied Satellite Navigation Using GPS, Galileo, and Augmentation Systems", Artech House, 2005.
- [3] W. B. Hofmann, H. Lichtenegger, and J. Collins, "GPS Fifth, revised edition", 2001.
- [4] D. K. Elliott, "Understanding GPS : Principles and Applications", Artech House, 1996.
- [5] W. Jinling, G. Matthew, L. Andrew, J. W. Jack, H. Songlai, and S. David, "Intergration of GPS/INS/Vision Sensors to Navigate Unmanned Aerial Vehicles", The International Archives of the Photogrammetry, Remote Sensing and Spatial Information Sciences, 37, pp. 963-969, Beijing, 2008.
- [6] S. Godha and M. E. Cannon, "Integration of DGPS with a Low Cost MEMS-based Inertial Measurement Unit(IMU) for Land Vehicle Navigation Application", Proceedings of ION GPA-05, Institute of navigation, pp. 333-345, Long Beach, 2005.
- [7] A. Broggi, C. Caraffi, R. I. Fedriga, and P. Grisleri, "Obstacle Detection with Stereo Vision for Off-road Vehicle Navigation", Computer Vision and Pattern Recognition, IEEE Computer Society Conference on, 3, pp. 65-72, 2005.
- [8] Y. C. Lim, M. H. Lee, C. H. Lee, S. Kwon, and J. H. Lee, "Improvement of Stereo Vision-based Position and Velocity Estimation and Tracking using a Strip-based Disparity Estimation and Inverse Perspective Map-based Extended Kalman Filter", Optics and Lasers in Engineering, 48, 9, pp. 859-868, 2010.

- [9] M. Bertozzi, A. Broggi, M. Cellario, A. Fascoli, P. Lombardi, and M. Porta, "Artificial Vision in Road Vehicles", *Proceeding of the IEEE*, 90, 7, pp. 1258-1271, 2002.
- [10] N. Srinivasa, "A Vision-based Vehicle Detection and Tracking Method for Forward Collision Warning", *IEEE Intelligent Vehicle Symposium*, pp. 626-631, 2002.
- [11] V. LEMONDE and M. DEVEY, "Obstacle Detection with Stereo Vision", *Mechatronics and Robotics*, Germany, 2004.
- [12] E. J. Rossetter, J. P. Switkes, and J. C. Gerfes, "Experimental Validation of the Potential Field Lanekeeping System", *International journal of automotive technology*, 5, 95, 2004.
- [13] R. Havard and H. Leonhard, "Gaussian Markov Random Fields", 2007.